

OPEN ACCESS

EDITED BY Lucian Copolovici, Aurel Vlaicu University of Arad, Romania

REVIEWED BY

Dhouha Belhadj Sghaier, National Institute of Marine Sciences and Technologies, Tunisia Dharam C. Attri, Islamic University of Science and Technology, India

*CORRESPONDENCE
Xian Xie
Xiexian@lcu.edu.cn

RECEIVED 02 September 2025 ACCEPTED 24 October 2025 PUBLISHED 26 November 2025

CITATION

Wang T, Dong C, Wan H, Zou R, Ren R, Yu S and Xie X (2025) Coordination between water source partitioning and isohydric-anisohydric behavior shapes contrasting water use strategies of *Tamarix chinensis* and *Ulmus pumila* in saline-alkaline soils. *Front. Plant Sci.* 16:1697666. doi: 10.3389/fpls.2025.1697666

COPYRIGHT

© 2025 Wang, Dong, Wan, Zou, Ren, Yu and Xie. This is an open-access article distributed under the terms of the Creative Commons Attribution License (CC BY). The use, distribution or reproduction in other forums is permitted, provided the original author(s) and the copyright owner(s) are credited and that the original publication in this journal is cited, in accordance with accepted academic practice. No use, distribution or reproduction is permitted which does not comply with these terms.

Coordination between water source partitioning and isohydric-anisohydric behavior shapes contrasting water use strategies of *Tamarix chinensis* and *Ulmus pumila* in saline-alkaline soils

Ting Wang¹, Chenguang Dong¹, Hui Wan¹, Rongsong Zou², Ranran Ren³, Shouchao Yu¹ and Xian Xie^{1*}

¹College of Agriculture and Biology, Liaocheng University, Liaocheng, Shandong, China, ²Comprehensive Experimental Center in Yellow River Delta of Chinese Academy of Forestry, Dongying, Shandong, China, ³Shandong Academy of Forestry, Jinan, Shandong, China

Plant water-use strategies are key functional traits for survival in water-limited ecosystems. Understanding how water uptake coordinates with physiological characteristics in coastal saline-alkaline environments is crucial for explaining drought adaptation. However, the specific responses of these strategies to water stress in such ecosystems remain unclear. In this study, we used hydrogen and oxygen stable isotope (δ^2 H and δ^{18} O) combined with a MixSIAR model to quantify seasonal variations in water uptake patterns of Tamarix chinensis and Ulmus pumila in the Yellow River Delta, China. Concurrently, we measured key physiological parameters, predawn and midday leaf water potential (Ψ_{pd} , Ψ_{md}) and stomatal conductance (g_s), to assess their iso-/anisohydric behavior. Redundancy analysis (RDA) was further used to explore the coordination between water uptake patterns and iso-/anisohydric strategies. T. chinensis exhibited a plastic water uptake strategy, adjusting water sources with seasonal aridity, and showed anisohydric behavior characterized by larger $\Delta\Psi$ and weak g_s sensitivity. In contrast, U. pumila maintained a conservative strategy, relying mainly on middle (33%) and deep soil water (31%) throughout the season and displayed isohydric behavior by tightly regulating g_s under declining Ψ_{md} . The distinct water uptake patterns of both species were tightly coordinated with their respective iso-/anisohydric behaviors and associated physiological traits. Anisohydric plasticity in T. chinensis provides greater adaptability to variable precipitation, whereas the conservative isohydric strategy of *U. pumila* may reduce drought resilience. These insights can guide species selection and management to improve drought tolerance in saline-alkaline coastal plantations.

KEYWORDS

stable isotope, water source partitioning, MixSIAR model, iso/anisohydric behavior, water-use strategy, saline-alkaline soil

1 Introduction

Water availability serves as a critical determinant of vegetation growth, structure, and function in forest ecosystems (Li et al., 2022). However, forest ecosystems of coastal saline-alkaline soils face acute hydrological constraints, where seawater intrusion elevates soil and groundwater salinity, imposing severe physiological restrictions on plant development (Zhang et al., 2022; Zhu et al., 2022). Furthermore, climate-induce precipitation variability amplifies spatiotemporal heterogeneity in water availability, exacerbating the scarcity of already limited water supplies (Gessler et al., 2022; He et al., 2024). These compounding pressures inevitably intensify vegetation degradation within forest ecosystems of saline-alkaline soils (Ewe et al., 2007). The survival and growth of trees under extreme environmental variability predominantly depend on their water-use strategies and physiological characteristics (Grossiord et al., 2017; Ding et al., 2021; Bachofen et al., 2024; Morgan et al., 2025). In this context, it is a priority to better understand how plant water use strategies will be affected in the future, which improve our ecohydrological understanding of biosphere-atmosphere feedbacks and associated climate change.

The spatial and temporal dynamics in water sources absorbed by plants are generally described as water uptake patterns (Wang et al., 2017). Root water uptake is a critical drought avoidance mechanism in arid or seasonally dry habitats because it helps sustain transpiration, photosynthesis, and survival under limited precipitation and strong evaporative demand (Zhao et al., 2020; Miguez-Macho and Fan, 2021; Bachofen et al., 2024). When rainfall is scarce, deep-rooted species often shift to deeper soil layers or groundwater to meet water demand (Liu et al., 2019; Wang et al., 2022; He et al., 2024; Zhang et al., 2024). Many studies have highlighted that accessing deep water provides a competitive edge in drought-prone environments (Barbeta et al., 2015; Yang et al., 2015). In coastal saline-alkaline soils, however, salinity also exerts a strong influence on plant water uptake (Min et al., 2019; Zhang et al., 2022). Previous research shows that halophytes can draw from deeper saline soil water or groundwater, whereas non-halophytes mainly rely on low-salinity soil water or rain-derived moisture stored in the surface soil (Zhu et al., 2022). Therefore, water uptake strategies represent a crucial functional trait for enhancing plant persistence during extended droughts in plantations of salinealkaline soils.

Variations in soil moisture regulate both the utilization of water sources and key physiological processes in trees, such as leaf water potential (Ψ) and stomatal conductance (g_s) (Martín-Gómez et al., 2017; Ding et al., 2021; Zhao et al., 2021). The Ψ and g_s dynamics in sustainable forest management under global change pressures has established the isohydric/anisohydric framework as a pivotal diagnostic tool. This classification system originates from observed interspecific differences in Ψ regulation capacity under fluctuating soil water availability, whether during seasonal variations or prolonged drought (Hochberg et al., 2018). Isohydric species employ stringent stomatal optimization to minimize transpiration water loss, thereby maintaining minimal diurnal Ψ fluctuations, effectively preventing xylem cavitation-

induced hydraulic failure. Conversely, anisohydric species exhibit transpiration patterns closely coupled with soil moisture dynamics, lacking defined minimum Ψ thresholds and consequently demonstrating greater $\Delta\Psi$ amplitudes (Martínez-Vilalta and Garcia-Forner, 2017; Walthert et al., 2024). Moreover, anisohydric species may exhibit greater drought resistance, likely linked to access to deeper and more stable water sources (Meinzer et al., 2016; Ding et al., 2021). However, understanding the possible iso/anisohydric behaviors of halophytic and non-halophytic plants in coastal saline-alkali ecosystems have received little attention. More importantly, the coordination between water source partitioning and isohydric-anisohydric behavior as possible adaptive responses to fluctuations in soil water availability remains unclear, especially in coastal saline-alkali soils.

Tamarix chinensis is a perennial deciduous shrub or small tree and a primary constructive species of saline-alkali land of the Yellow River Delta. T. chinensis develops roots, which can enrich soil salinity and reduce soil pH (Chen et al., 2022). In addition, it contributes to soil improvement, acts as a windbreak, stabilizes sand, attenuates waves, and facilitates silt deposition. Extensive natural stands of T. chinensis occur in the tidal flats of the Yellow River Delta, where they play a vital role in enhancing the ecological environment and sustaining the stability of ecosystems (Sun et al., 2023). Ulmus pumila is a deciduous broadleaf tree species extensively utilized in ecological restoration efforts across the Yellow River Delta. In recent years, owing to the extensive exploitation of groundwater in the local area, seawater intrusion has resulted in soil salinization, and the ratio of evaporation to precipitation has escalated. Due to the shortage of freshwater resources, salt-alkali and drought stresses have emerged as the two major factors influencing the growth of vegetation in the local area. Therefore, elucidating the water use strategies of dominate species in coastal saline-alkali ecosystems constitutes a critical imperative for developing targeted mitigation measures against vegetation degradation. In this study, we used stable hydrogen and oxygen isotopes ($\delta^2 H$ and $\delta^{18}O$) to examine seasonal water uptake patterns and physiological response, in a mixed forest of T. chinensis and U. pumila in the Yellow River Delta region. We further discerned the iso/anisohydric behaviors of T. chinensis and U. pumila and coordinated them with their water uptake patterns. We addressed the following three questions: (1) Do T. chinensis and U. pumila exhibit distinct water use patterns? (2) What are the isohydric versus anisohydric behaviors of *T. chinensis* and U. pumila? (3) How does the coordination between water source partitioning and isohydric-anisohydric behavior shape the adaptation of T. chinensis and U. pumila to water limitations in saline-alkaline soils?

2 Materials and methods

2.1 Study area and experimental design

This study was conducted in Comprehensive Experimental Center in Yellow River Delta of Chinese Academy of Forestry

(118° 54′ E, 37°41′ N), which is situated in Dongying City, Shandong Province in east of China. The region experiences a warm-temperate monsoonal climate, characterized by pronounced seasonality. The region has a mean annual temperature of 12.4°C and receives 550 mm of precipitation annually. Rainfall is unevenly distributed, with approximately 70–80% occurring during the growing season from May to September. The soils are coastal saline-alkaline. Vegetation is dominated by xerophytic and halophytic species, along with shrubs and herbaceous plants.

Tamarix chinensis and Ulmus pumila are two dominant species in the local vegetation communities. These plantations were established around 2020 through the transplantation of two-yearold seedlings. This stand age represents a critical window of high physiological plasticity, during which water-use strategies are fundamental to species adaptation in saline-alkaline environments. The root architectures are clearly different between two woody species. In the saline-alkali soils of the Yellow River Delta, U. pumila exhibits a laterally extensive shallow root system, with over 80% of its fine roots concentrated within the upper 0.8m of the soil profile. In contrast, Tamarix chinensis develops a vertically oriented root architecture, with a mean maximum root depth of 1.2m. Three mixed forest plots (20m × 20m) were established on flat terrain in the Yellow River Delta, where T. chinensis and U. pumila are the dominant woody species. The stands are characterized by a mixed canopy with a density of approximately 5000 trees per hectare, with a species mix ratio of about 70% T. chinensis and 30% U. pumila. The understory was sparse, dominated by shallow-rooted herbaceous species such as Phragmites australis, Cynanchum chinense, Imperata cylindrica, Aeluropus sinensis.

2.2 Sample collection

From April to September 2024, soil, plant, rainwater, and groundwater samples were collected monthly. Rainwater was collected after each precipitation event using polyethylene bottles with funnels placed in an open area adjacent to the forest, and rainfall amounts were measured with a rain gauge. For each species, three individuals per plot were selected for xylem sampling on each sampling date. To minimize isotopic fractionation and avoid contamination by enriched water, the phloem tissue of T. chinensis and U. pumila was removed prior to analysis (Dawson and Pate, 1996). Plant samples were cut into 3-4 cm segments, sealed in screw-cap glass vials wrapped with Parafilm, and immediately frozen (-16°C) for isotope analysis. Soil samples were collected at the same time as plant tissues using a petrolpowered auger at five depths (0-20, 20-40, 40-60, 60-80, and 80-100 cm). Each soil sample was divided into two portions: one stored frozen for isotope analysis, and the other oven-dried at 80 °C to constant weight for determining gravimetric soil water content (SWC, %). Furthermore, soil electrical conductivity (EC) was determined using a 1:5 soil:water suspension and showed significant vertical stratification, with values of 1.60 \pm 0.07, 1.23 \pm 0.25, 1.11 ± 0.05 , 0.72 ± 0.09 , and 1.11 ± 0.08 dS m⁻¹ for the 0-20, 20–40, 40–60, 60–80, and 80–100 cm soil layers, respectively. Groundwater was sampled from a 2m deep well located ~200 m from the plots. To prevent isotopic alteration, all samples were sealed in glass vials with Parafilm immediately after collection and stored at -16° C until analysis.

2.3 Stable isotopic analyses

Water from soil and plant xylem samples was extracted via cryogenic vacuum distillation. The stable isotope compositions ($\delta^2 H$ and $\delta^{18} O$) of rainwater, soil water, xylem water, and groundwater were determined using an isotope ratio mass spectrometer (Delta V Advantage, Thermo Fisher Scientific, Waltham, MA, USA) coupled with an elemental analyzer (Flash 2000 HT, Thermo Fisher Scientific). The analytical precision was $\pm 1\%$ for $\delta^2 H$ and $\pm 0.2\%$ for $\delta^{18} O$. Isotope ratios were calculated according to Equation 1:

$$\delta = \left[\left(R_{\text{sample}} / R_{\text{standard}} \right) - 1 \right] \times 1000\% \tag{1}$$

where R_{sample} and $R_{standard}$ denoted the $^2H/^1H$ and $^{18}O/^{16}O$ molar ratio of the sample and the V-SMOW (Vienna Standard Mean Ocean Water) standards, respectively.

2.4 Hydrogen isotopic offset correction

Stable water isotopes (δ^{18} O and δ^{2} H) are widely used to investigate plant water uptake strategies. Their application in plant-water relations assumes that no isotopic fractionation occurs during water absorption in terrestrial plants (Dawson and Ehleringer, 1991; Ehleringer and Dawson, 1992). However, δ²H fractionation has been observed in root water uptake for certain halophyte and xerophyte species, leading to $\delta^2 H$ offsets (Lin and Sternberg, 1993). To evaluate potential isotopic offsets between plant xylem water and its sources, the concepts of lineconditioned excess (LC-excess) and soil water excess (SW-excess) have been proposed by Landwehr and Coplen (2006) and further developed by Barbeta et al. (2019), respectively. In this study, groundwater, in addition to soil water, was considered an important water source, particularly in areas with shallow water tables. Therefore, a potential water line (PWL) was constructed by linear regression of soil water and groundwater isotope data (Li et al., 2021). The δ^2 H deviation of stem water from the PWL (PWexcess) was calculated as Equation 2:

$$PW - excess = \delta^2 H - a_p \delta^{18} O - b_p$$
 (2)

where a_p and b_p are the slope and intercept of the PWL, respectively. Positive PW-excess values indicate that stem water δ^2 H is enriched relative to the PWL, with larger values reflecting greater enrichment. Conversely, negative PW-excess values indicate depletion, with more negative values representing greater depletion. A PW-excess of zero indicates no δ^2 H offset between stem water and the PWL. The validity of the PW-excess correction was assessed

by verifying that the corrected xylem water isotopes fell within the mixing polygon defined by the potential sources (soil water and groundwater). Stem water $\delta^2 H$ values were corrected by subtracting the corresponding PW-excess from the original measurements and these corrected values were used in subsequent MixSIAR analysis.

2.5 Determination the plant water sources

The proportion of plant water uptake from each source was estimated using the Bayesian mixing model (MixSIAR), which accounts for uncertainty in root water absorption and provides a single optimal solution rather than a range of feasible outcomes (Wang et al., 2017; Zhang et al., 2024). Accordingly, MixSIAR was employed to quantify the contributions of different potential water sources to the trees.

Stem water δ^2 H values, corrected by the PWL (i.e., subtracting PW-excess), together with δ^{18} O values, were used as the mixture data. Source data comprised the mean and standard error of soil water isotopes at various depths and groundwater. Isotope fractionation for both $\delta^2 H$ and $\delta^{18} O$ was assumed to be zero. The Markov chain Monte Carlo (MCMC) chain length was set to 'long', and convergence was assessed using Gelman-Rubin and Geweke diagnostics. In the model, the error structure was specified as 'Residual only', and the prior was set to 'uninformative/ Generalist' (Wang et al., 2017). Model performance was evaluated using the Akaike information criterion (AIC), Bayesian information criterion (BIC), and root mean square error (RMSE), with the dataset yielding the lowest AIC, BIC, and RMSE selected as the optimal input. The analyses were performed with MixSIAR package in R software (Stock and Semmens, 2013). To accurately capture the main zones of root activity and water uptake, the water sources from different soil layers were combined into shallow (0-20 cm), middle (20-60 cm) and deep (60-100 cm) soil layers to facilitate the subsequent analysis and comparison (Liu et al., 2019).

2.6 Leaf gas exchange and water potential measurements

Leaf water potential (Ψ) and photosynthetic performance were monitored from April to September 2024. Photosynthetic parameters were measured using a gas-exchange system (Li-6400; LiCOR Inc., Lincoln, NB, USA) with a 2cm × 3cm light-source cuvette, between 09:00 and 11:00 on cloudless days in the middle of each month. For each tree, three branches were selected, and three to five fully expanded leaves per branch were measured. Net photosynthetic rate (A_n , μ mol m⁻² s⁻¹), transpiration rate (T_r , mmol m⁻² s⁻¹), and stomatal conductance (g_s , mol m⁻² s⁻¹) were calculated on a leaf area basis. Predawn (Ψ_{pd} , MPa) and midday (Ψ_{md} , MPa) leaf water potentials were determined *in situ* using a Psypro plant water potential meter (WESCOR, USA) at 05:00–06:00 and 12:00–13:00, respectively, on sunny days in the middle of each month. Measurements were conducted on the same branches and leaves used for photosynthetic assessments.

2.7 Statistical analysis

Data were analyzed using two-way ANOVA analysis to examine the effects of species (T. chinensis, U. pumila), season (dry, wet), and their interaction on $\delta^2 H$ and $\delta^{18} O$ values and physiological variables, followed by multiple comparisons at p < 0.05 level of significance. Ordinary least squares (OLS) regression was employed to quantify bivariate correlations among physiological traits within each species. For multivariate analysis, redundancy analysis (RDA) was performed to evaluate the joint relationship between leaf water potential, stomatal conductance, net photosynthetic rate, transpiration rate, soil water content, and root water uptake proportion with vegan package in R software. All statistical analyses were performed with R 4.3.2.

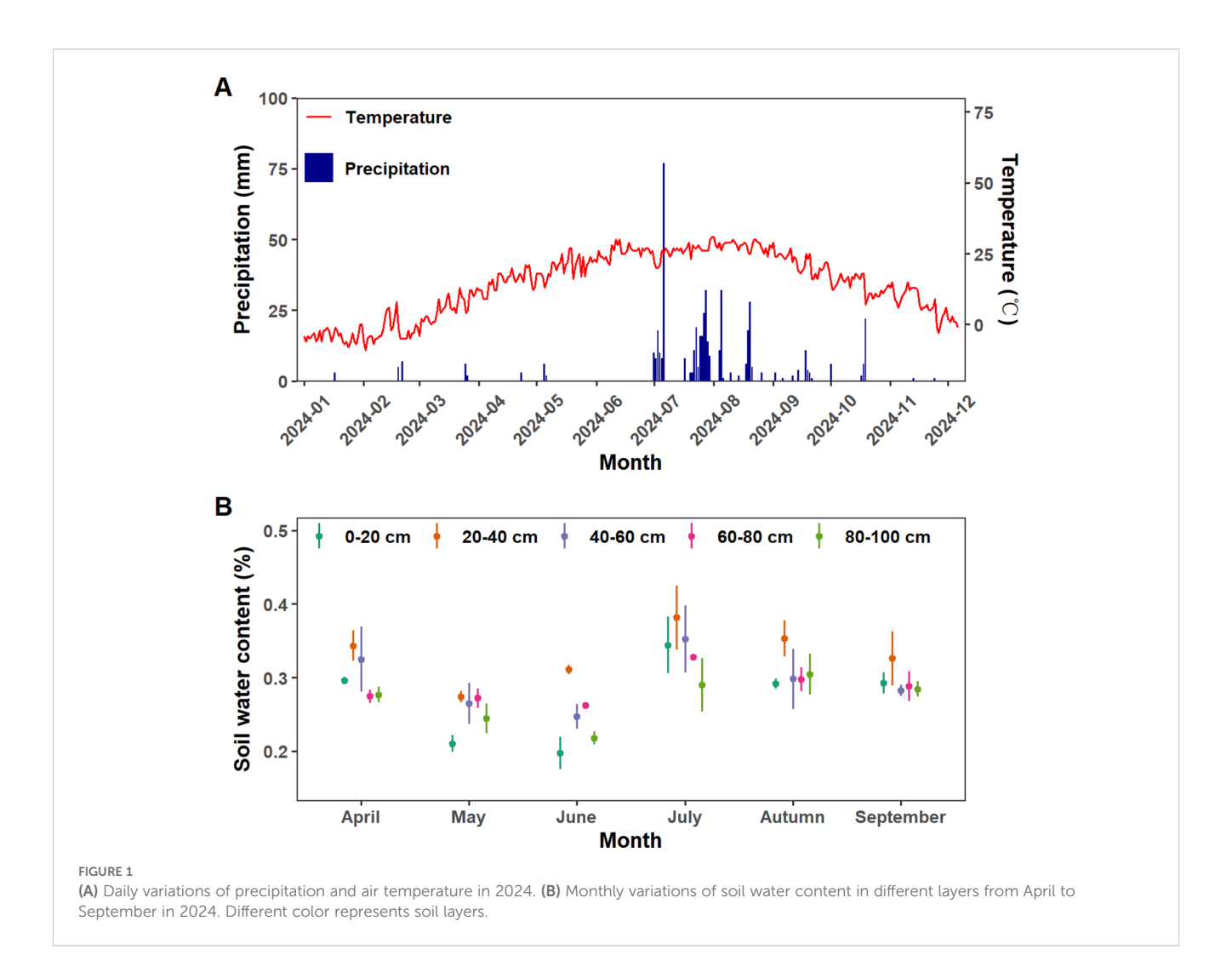
3 Results

3.1 Hydrometeorological parameters

The total precipitation was 662.5mm during the observation period in 2024 (Figure 1A), with pronounced seasonal variations (p< 0.01). The accumulated monthly precipitation during April to September was 3.0mm, 8.0mm, 0mm, 291.0mm, 270.5mm and 29.0mm, respectively (Figure 1A). Similarly, SWC exhibited distinct seasonal dynamics, progressively decreasing to its lowest level between April and June, sharply increasing in July, and subsequently declining (Figure 1B). This precipitation pattern, combined with the dynamics of SWC, defined distinct dry (April-June) and wet (July-September) seasons (Figure 1). The surface layer (0-20 cm) exhibited the lowest mean SWC (27.20 \pm 5.57%) but highest temporal variability. Middle soil layers (20-60 cm) exhibit the highest SWC in over the entire growing season, and it was significantly influenced by seasonal variations. Although deeplayer soil moisture (60-100 cm) exhibited the highest stability, it was still significantly influenced by seasonal alternations between dry and wet periods (p<0.05).

3.2 Variations in the proportion of plant water uptake

Precipitation $\delta^2 H$ and $\delta^{18} O$ values were distributed along a line with a slope of 8.25 and an intercept of 11.26, representing the local meteoric water line (LMWL) (Figure 2). Most soil water samples plotted to the lower right of the LMWL, forming a soil water line (SWL) with a slope of 2.41 (Figure 2). Across the growing season, surface soil water was significantly more enriched than deeper layers (p<0.05 for both isotopes), reflecting evaporative effects at the soil surface (Figure 2). The isotopic signatures of U. pumila closely aligned with those of soil water, suggesting that it primarily utilized water from different soil depths (Figure 2B). By contrast, the isotopic values of T. chinensis fell outside the soil mixing space, indicating potential hydrogen isotope fractionation during water uptake (Figure 2A).

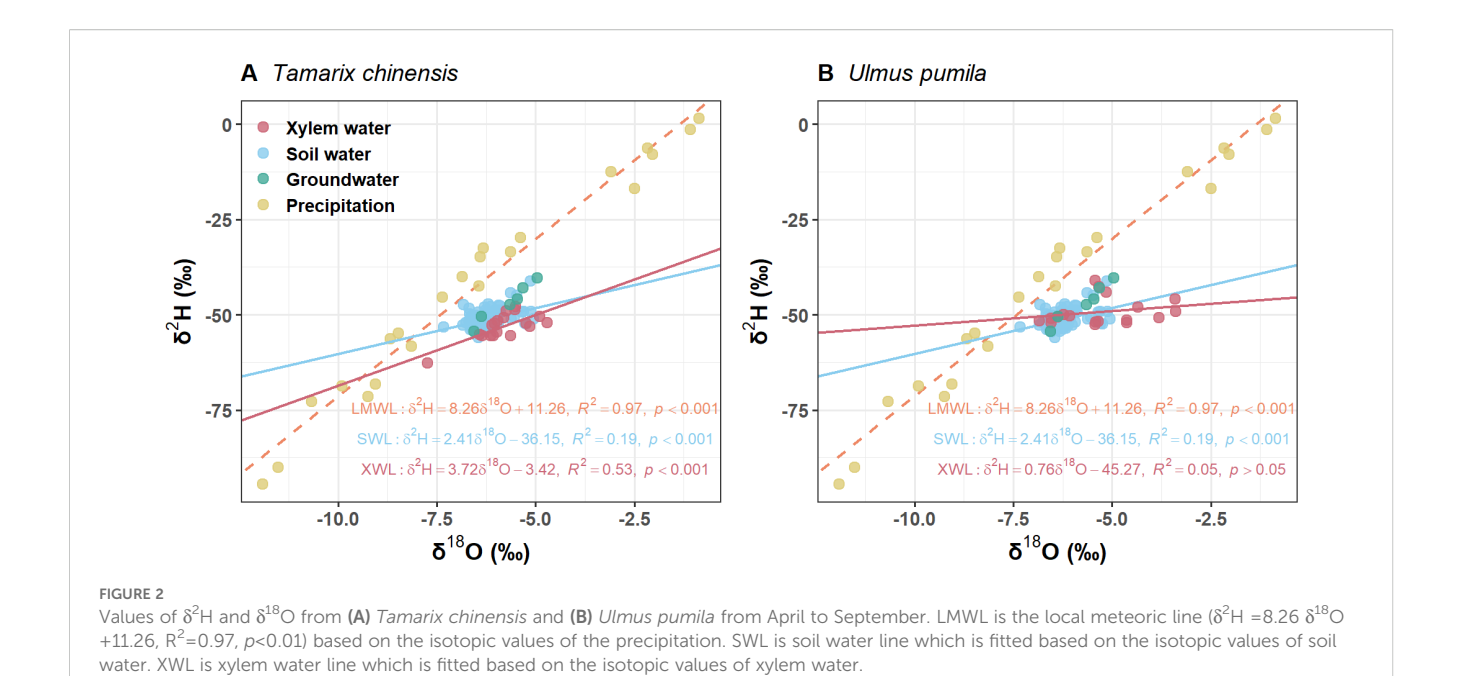


Dual-isotope (δ^2 H and δ^{18} O) with MixSIAR modeling revealed contrasting water uptake patterns between T. chinensis and U. pumila (Figure 3). T. chinensis exhibited marked seasonal shifts in water source partitioning. It primarily relied on shallow and intermediate soil water during the early growing season (61% and 60% in April and May, respectively), but progressively increased deep soil water and groundwater utilization to 54% in June and 72% in July as drought intensity escalated (Figure 3A). In wet season (August-September), T. chinensis tend to uptake water from intermediate and deep soil water, with the contributions rebounding to 48% and 72%, respectively (Figure 3A). In contrast, U. pumila maintained stable reliance on intermediate (33%) and deep (31%) soil layer water throughout the growing season, with limited groundwater exploitation (14%, Figure 3B). Collectively, T. chinensis employs a plastic water uptake strategy, dynamically shifting soil water acquisition depths in response to seasonal drought, whereas U. pumila maintains a conservative water-use pattern characterized by stable dependence on middle and deep soil water throughout the growing season.

3.3 Estimates of isohydric and anisohydric behavior

T. chinensis and U. pumila exhibited contrasting water use strategies (Figure 4; Table 1). T. chinensis exhibited higher A_n than U. pumila in dry season (May), but lower A_n in wet season (September; Figure 4). g_s in T. chinensis was significantly 32% higher than U. pumila during dry season (April–June), with no divergence in the wet season (July-September; Figure 4B). Similarly, T_r was significantly 41% greater in T. chinensis than in U. pumila under drought stress (Figure 4C). Although both species showed comparable Ψ_{pd} (Figure 4D), T. chinensis maintained significantly lower Ψ_{md} than U. pumila across growing season (Figure 4E). Similarly, the $\Delta\Psi$ was significantly smaller in T. chinensis than in U. pumila during growing season (Figure 4F), highlighting their fundamentally divergent water-use strategies.

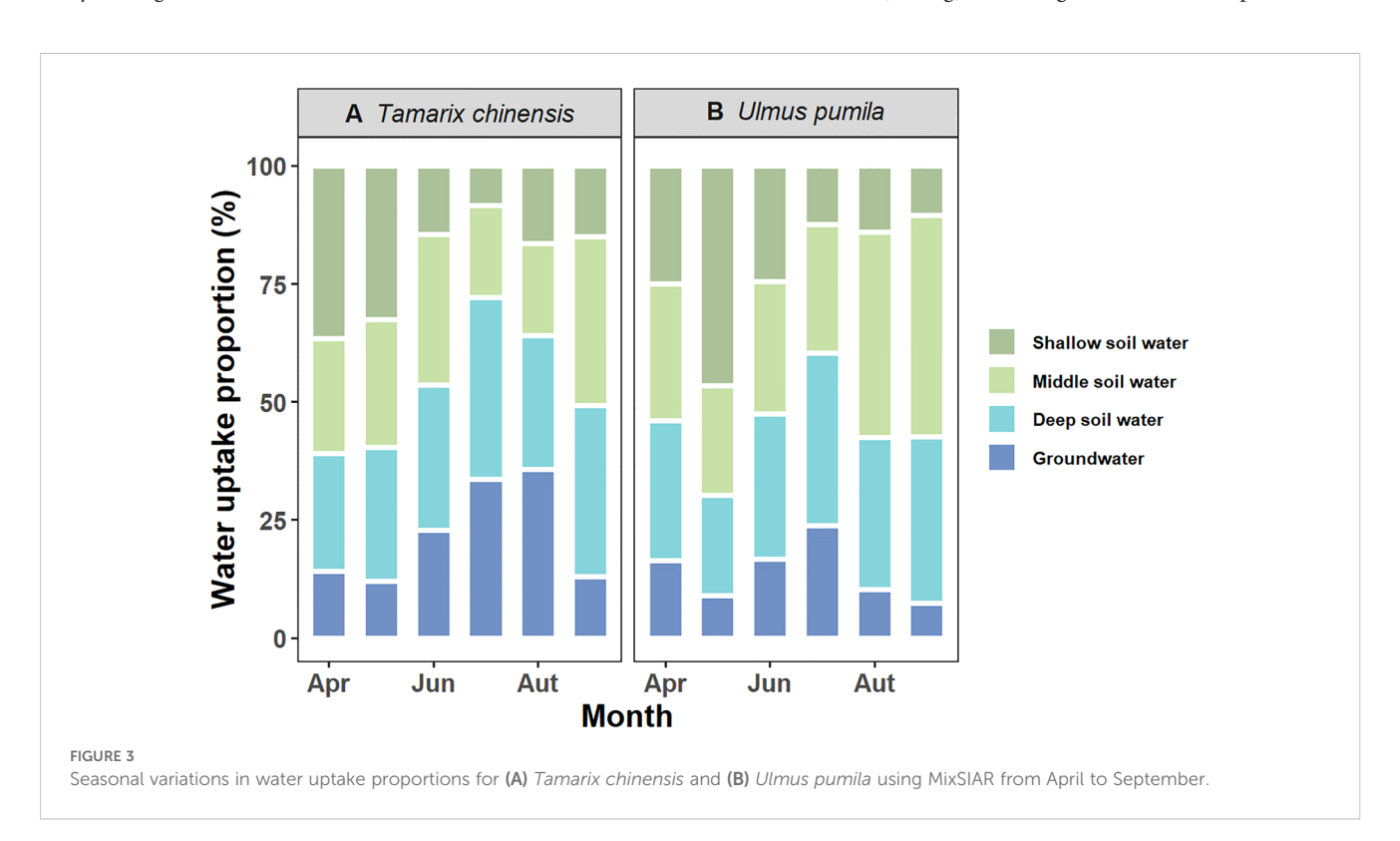
Crucially, *T. chinensis* and *U. pumila* exhibited contrasting isohydric and anisohydric behaviors, evident in their water potential regulation (Figure 5). For *U. pumila*, Ψ_{pd} positively

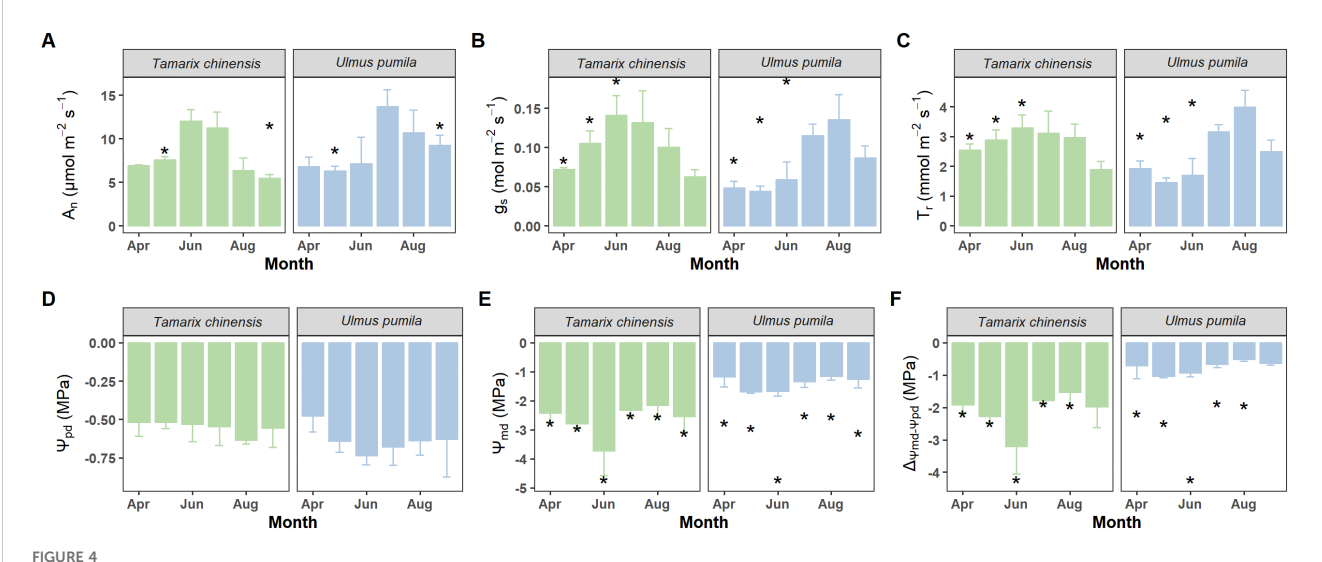


correlated strongly with Ψ_{md} ($R^2=0.68, p<0.05$; Figure 5E), and $\Delta\Psi$ increased significantly with g_s ($R^2=0.30, p<0.05$; Figure 5F), collectively demonstrating tight stomatal regulation of leaf water status characteristic of isohydric behavior. In contrast, *T. chinensis* showed no correlation between Ψ_{pd} and Ψ_{md} (Figure 5C) or between g_s and $\Delta\Psi$ (Figure 5D). These distinct hydraulic responses confirm that *T. chinensis* demonstrates strong anisohydric behavior, while *U. pumila* exhibits characteristic isohydric regulation.

3.4 Water uptake depth coordinated with iso/anisohydric behavior

RDA revealed that the main components explained 60.68% and 43.57% of the total variance in water source utilization for *T. chinensis* and *U. pumila*, respectively (Figure 6), highlighting the coordination of physiological characters and water uptake patterns. For *T. chinensis*, g_s , Ψ_{md} , and C_i collectively dominated water uptake variations, with reductions in Ψ_{md} and g_s correlating with increased dependence on





Monthly variations of net photosynthetic rate (A_n, **A**), stomatal conductance (g_s, **B**), transpiration rate (T_r, **C**), predawn leaf water potential (Ψ_{pd} , **D**), midday leaf water potential (Ψ_{md} , **E**) and the difference between midday and predawn leaf water potential ($\Delta_{\Psi_{md}-\Psi_{pd}}$, **F**) for *Tamarix chinensis* and *Ulmus pumila* from April to September 2024. The asterisks on the columns indicate that there are significant differences in the physiological characteristics of *Tamarix chinensis* and *Ulmus pumila* at p<0.05. Error bars express as standard deviation.

deep soil water (Figure 6A). In contrast, U. pumila exhibited stronger coupling between A_n , T_r , g_s and SWC, where maintained middle and deep soil water utilization corresponded to high A_n and T_r and SWC availability (Figure 6B). This indicates U. pumila maintained water source utilization despite constrained photosynthetic assimilation. Collectively, water source partitioning is coordinate with isohydricanisohydric behavior of T. chinensis and U. pumila in salinealkaline soils.

4 Discussion

4.1 Differences in water uptake patterns between *T. chinensis* and *U. pumila*

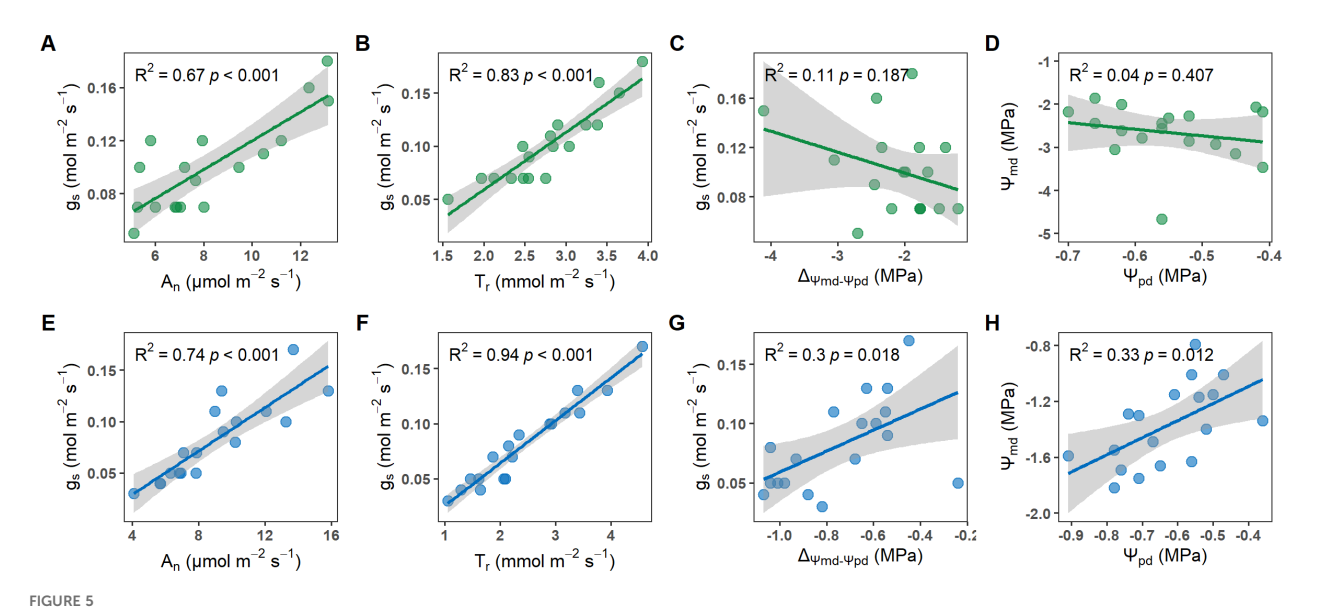
Understanding the water uptake patterns influencing drought vulnerability is crucial for effective forest management and

vegetation restoration strategies (Miguez-Macho and Fan, 2021; Bachofen et al., 2024; He et al., 2024; Wang et al., 2024). Isotope mixing models revealed contrasting water uptake pattern between T. chinensis and U. pumila (Figure 3). U. pumila exhibited a conservative strategy with minimal seasonal variation, predominantly relying on stable middle and deep soil water throughout the growing season (Figure 3). This may attribution that soil salinity plays a key role in shaping plant water uptake strategy in saline-alkaline soils (Zhang et al., 2022; Zhu et al., 2022). Surface soil water is prone to rapid evaporation, leading to salt accumulation in upper layers (Xia et al., 2019; Lei et al., 2025). Meanwhile, groundwater in the study area exhibited high salinity levels, which can inhibit root penetration due to osmotic stress (Sun et al., 2022). As a result, U. pumila roots tend to avoid both the saline surface layer and the high-salinity groundwater, further reinforcing their dependence on middle and deep soil water. This avoidance strategy reflects a form of vertical confinement, where the

TABLE 1 Xylem water isotopes and physiological traits of Tamarix chinensis and Ulmus pumila across dry (April-June) and wet (July-September) seasons.

Parameter	Dry season		Wet season	
	Tamarix chinensis	Ulmus pumila	Tamarix chinensis	Ulmus pumila
δ²Η (‰)	-54.63 ± 1.17 Ab	-50.43 ± 0.75 Aa	-51.55 ± 0.91 Aa	-48.17 ± 1.43 Aa
δ ¹⁸ O (‰)	-5.72 ± 0.30 Ab	-4.49 ± 0.27 Aa	-5.94 ± 0.10 Aa	-6.06 ± 0.20 Ba
$A_n (\mu mol m^{-2} s^{-1})$	8.83 ± 0.83 Aa	6.75 ± 0.56 Bb	7.70 ± 0.98 Ab	11.21 ± 0.88 Aa
T _r (mmol m ⁻² s ⁻¹)	2.90 ± 0.15 Aa	1.69 ± 0.13 Bb	2.65 ± 0.25 Aa	3.21 ± 0.25 Aa
g _s (mol m ⁻² s ⁻¹)	0.10 ± 0.01 Aa	0.05± 0.01 Bb	0.10 ± 0.01 Aa	0.11 ± 0.01 Aa
Ψ _{pd} (MPa)	-0.52 ± 0.03 Aa	-0.62 ± 0.04 Aa	-0.58 ± 0.03 Aa	-0.65 ± 0.05 Aa
Ψ _{md} (MPa)	-2.98 ± 0.25 Bb	-1.51 ± 0.10 Aa	-2.34 ± 0.13 Ab	-1.25 ± 0.07 Aa

Different uppercase letters indicate significant differences between seasons (p<0.05), and different lowercase letters indicate significant differences between species within the same season (p<0.05). Values are presented as mean \pm SE.

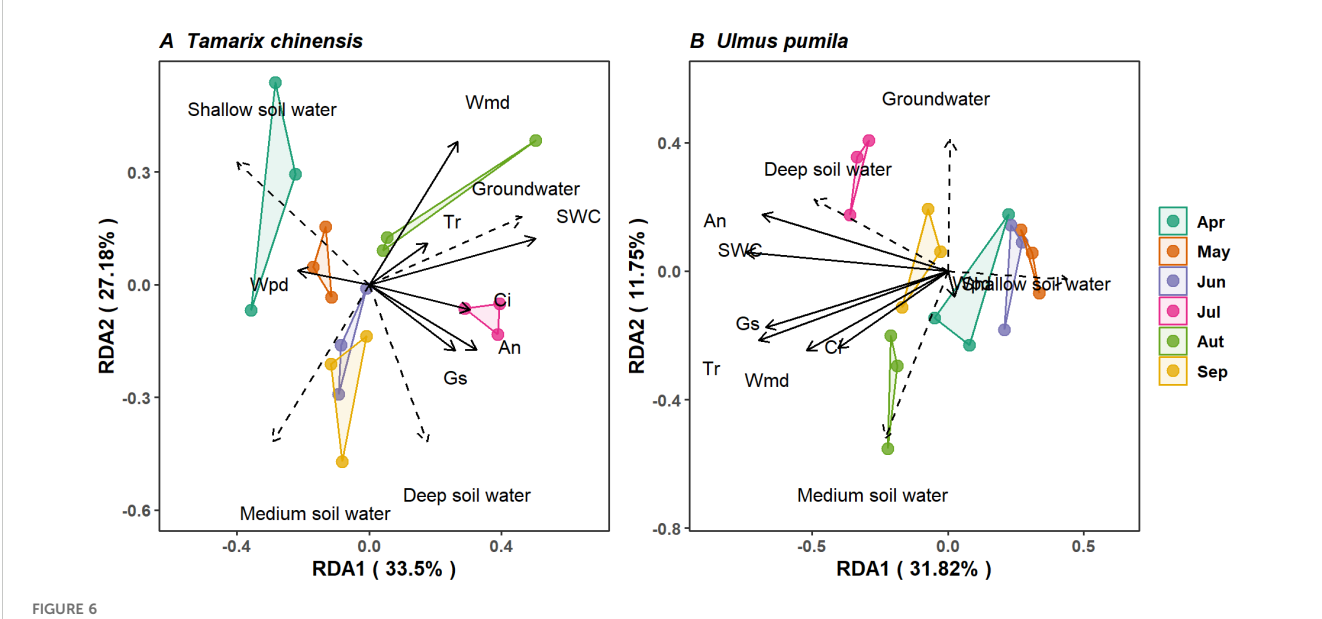


Relationship between stomatal conductance (g_s) and net photosynthetic rate $(A_n; \mathbf{A}, \mathbf{E})$, stomatal conductance (g_s) and transpiration rate $(T_r; \mathbf{B}, \mathbf{F})$, stomatal conductance (g_s) and the difference between predawn and midday leaf water potential $(\Delta \Psi; \mathbf{C}, \mathbf{G})$, predawn (Ψ_{pd}) and midday leaf water potential $(\Psi_{md}; \mathbf{D}, \mathbf{H})$ for *Tamarix chinensis* and *Ulmus pumila* from April to September in 2024.

plant minimizes upward or downward root extension to evade salt stress, while maximizing horizontal spread within the favorable mid-soil zone (Sun et al., 2023). This "horizontal expansion-vertical limitation" pattern restricts the tree's ability to tap into deeper water reserves during prolonged droughts, potentially increasing its vulnerability under extreme water stress.

In contrast, *T. chinensis* demonstrated pronounced seasonal plasticity in water source partitioning. *T. chinensis* progressively increased reliance on deep soil water and groundwater relatively dry

conditions, but shifting to middle and deep soil water under wet conditions (e.g. August and September) (Figure 3). This pattern of water uptake aligns with earlier studies reporting that halophytes adjust their water sources between shallow and deep soils in response to changes in soil water availability (Sun et al., 2022; Zhu et al., 2022). Shifting in water uptake between shallow and deep soil layers are primarily determined by a species' root dimorphism (Yang et al., 2015; Wang et al., 2017; Liu et al., 2019). *T. chinensis* is one such species, with a root architecture composed of both shallow



Correlation between water uptake from each source and basic topography, soil properties for *Tamarix chinensis* (A) and *Ulmus pumila* (B) in redundancy analysis. Solid line denotes the explained variables. Ψ_{pd} is predawn leaf water potential; Ψ_{md} midday leaf water potential; $\Delta\Psi$ the difference between predawn and midday leaf water potential; g_s stomatal conductance; and A_n net photosynthetic rate, T_r transpiration rate and SWC soil water content.

and deep roots, allowing it to extract water from multiple soil layers depending on environmental conditions (Imada et al., 2015; Sun et al., 2022). Besides, *T. chinensis* uptake more high-salinity groundwater than *U. pumila*, demonstrating exceptional salt tolerance that facilitates root extension into saline aquifers. This ability to dynamically adjust water use in response to fluctuations in rainfall and soil moisture, characterized by a shift in uptake from shallow to deeper soil layers, reflects strong ecological plasticity, which is crucial for plant survival in variable and often harsh environments and is often associated with a greater capacity to adapt to changing conditions (Grossiord et al., 2017; Jiang et al., 2020; Gessler et al., 2022; Wang et al., 2022). Therefore, the differences in root distribution and salt tolerance underpin *T. chinensis*'s superior drought resistance.

4.2 Contrasting isohydric and anisohydric behavior between *U. pumila* and *T. chinensis*

Our findings demonstrate contrasting iso-/anisohydric behaviors between *U. pumila* and *T. chinensis*, which reflect their fundamentally different strategies for regulating plant water use under fluctuating environmental conditions. U. pumila exhibited a typical isohydric response, characterized by tight control of stomatal conductance. Specifically, we observed significant positive correlations between U. pumila g_s and Ψ_{md} ($R^2 = 0.33$, p=0.012; Figure 5H), as well as between g_s and the diurnal water potential difference ($\Delta \Psi$, $\Psi_{\rm md}$ – $\Psi_{\rm pd}$) (R²= 0.30, p=0.018; Figure 5G). This indicates that *U. pumila* conserves water during drought by closing stomata in response to declining leaf water potential, reflecting a classic isohydric strategy of transpiration control. Similar results suggested that some plant species employed an isohydric strategy based on daily changes in stomatal conductance and stem vulnerability (McDowell et al., 2008; Meinzer et al., 2016; Martín-Gómez et al., 2017). This reinforces the general understanding that isohydric plants adjust stomatal behavior to reduce water loss, with stomatal conductance responding directly to changes in water potential (Martínez-Vilalta and Garcia-Forner, 2017; Hochberg et al., 2018). In contrast, T. chinensis demonstrated an anisohydric behavior, as evidenced by the lack of significant correlation between g_s and $\Delta \Psi$ or Ψ_{md} (Figure 5C and D) and more negative $\Delta \Psi$ ($\Psi_{md} - \Psi_{pd}$) (Figure 4F). During dry months (April-June), T. chinensis maintained higher g_s and T_r than U. pumila (Figures 4B, C), despite exhibiting significantly lower Ψ_{md} (Figure 4E). This suggests that T. chinensis allows greater fluctuation in water potential while sustaining gas exchange, even under increasing drought intensity. Such behavior is adaptive in environments with temporally variable water availability, as it enables continuous carbon assimilation at the cost of increased risk of hydraulic failure (Hochberg et al., 2018; Xue et al., 2024).

Furthermore, seasonal variance in Ψ_{md} provided additional evidence of these divergent strategies. *T. chinensis* exhibited larger

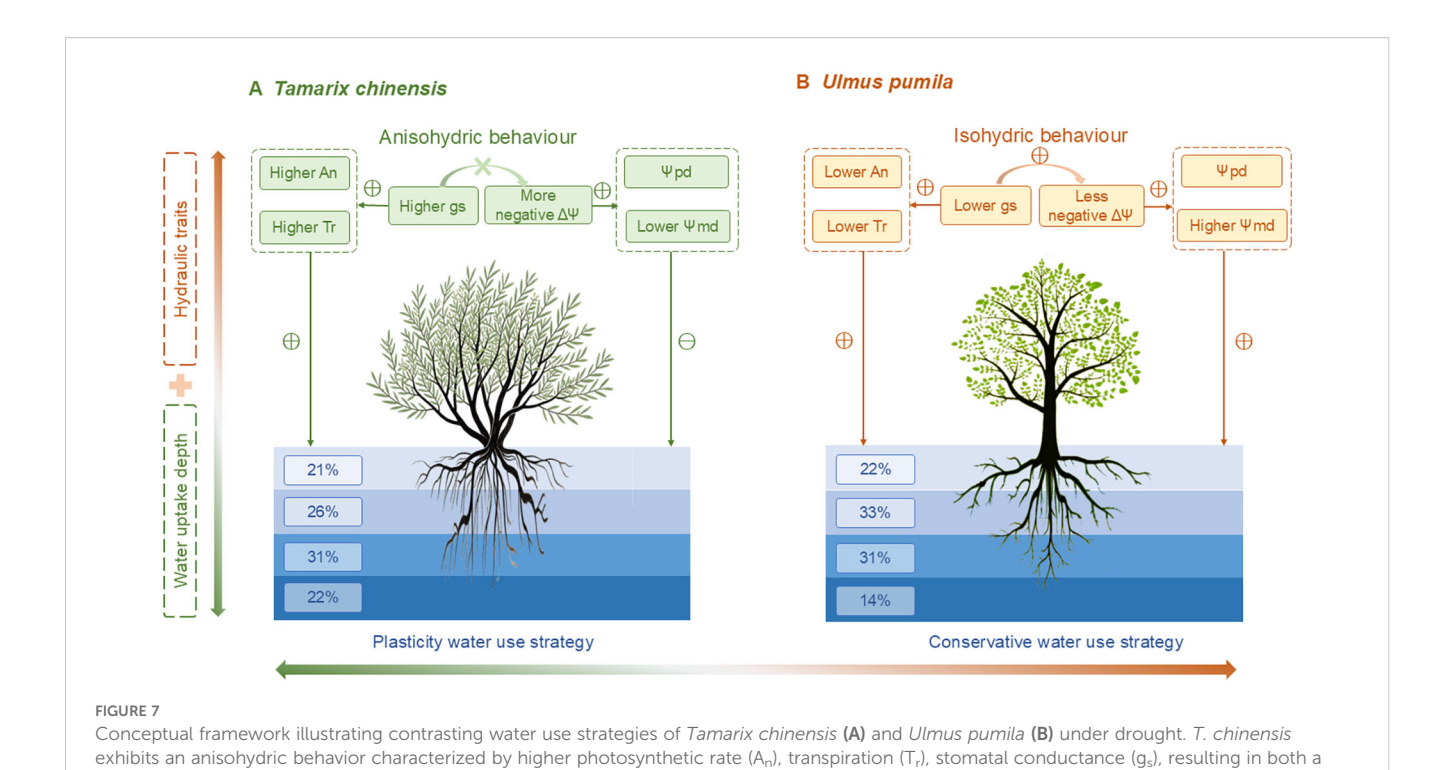
 $\Psi_{\rm md}$ values under drought, while *U. pumila* maintained smaller $\Psi_{\rm md}$ across seasons (Figure 4F). The sharp rebound in $\Psi_{\rm md}$ for T. chinensis in July, coinciding with the onset of the wet season, further indicates its capacity for rapid hydraulic recovery, consistent with anisohydric flexibility. This result aligns with Franks et al. (2007), who observed that Ψ_{md} in anisohydric plants exhibits seasonal fluctuations, highlighting the need to evaluate iso- and anisohydric behaviors across multiple temporal scales, as performed in the present study. Taken together, these results suggest that U. pumila adopts a conservative, water-saving approach under stress, prioritizing hydraulic safety, whereas T. chinensis tolerates more negative water potentials to maintain higher gas exchange, reflecting a riskier but potentially more productive strategy. This divergence in iso-/anisohydric behavior underpins each species' unique drought adaptation strategy in the saline-alkaline ecosystems of the Yellow River Delta.

4.3 Coordination between water uptake patterns and iso-/anisohydric behavior

The water uptake patterns of T. chinensis and U. pumila are tightly coordinated with their respective iso-/anisohydric behaviors and associated physiological traits (Figures 6, 7). Redundancy analysis (RDA) revealed that water uptake depth and physiological regulation co-vary in response to environmental conditions, suggesting a functional integration of water-use strategy and hydraulic traits (Figure 6). For *U. pumila*, the increased reliance on deep soil water was associated with higher Ψ_{md} , g_s , A_n , T_r and SWC (Figure 6B). These physiological traits, in coordination with isohydric regulation, constrain water source selection by limiting water uptake to relatively stable, less saline soil layers in order to maintain leaf water potential under drought conditions (Ding et al., 2021; Zhu et al., 2022). Although *U. pumila* demonstrates capacity to extract water from middle and deep soil layers, its limited salt tolerance and shallow root penetration inhibit its ability to exploit high-salinity groundwater in saline-alkaline environments. This physiological constraint likely restricts its drought resilience under prolonged or severe aridity.

In contrast, T. chinensis exhibited increased reliance on deep soil water during the dry season was associated with lower $\Psi_{\rm md}$ and higher $g_{\rm s}$ (Figure 6A). This response supports that anisohydric strategy, characterized by sustained stomatal opening and declining water potential, facilitates access to more stable, deeper water reserves (Kannenberg et al., 2019; Walthert et al., 2024). This physiological coordination supports the view that anisohydric regulation enhances the ecological plasticity of T. chinensis, allowing it to adjust water uptake in response to temporal changes in soil moisture. Indeed, our findings show that T. chinensis dynamically shifted its water source from shallow to deep layers as drought intensified (Figure 3A). The physiological traits support a flexible drought response strategy, maximizing water acquisition and gas exchange even under prolonged water deficits.

Therefore, our findings suggest that the coordination between iso-/anisohydric behavior and root water uptake strategy enables



more negative water potential difference ($\Delta\Psi$) and lower midday water potential (Ψ_{md}), which lead to greater plasticity in water uptake depth. In contrast, *U. pumila* shows an isohydric behavior with lower A_n , T_r , g_s , and a less negative $\Delta\Psi$, and higher Ψ_{md} , adopting a conservative water use strategy with relatively stable, middle soil water uptake. Hydraulic traits (upper panel) and water uptake depth proportions (lower panel) jointly

T. chinensis and U. pumila to adopt contrasting yet functional drought responses. T. chinensis exemplifies an anisohydric species with high physiological plasticity, able to flexibly shift water sources while maintaining gas exchange under stress. In contrast, U. pumila exemplifies a conservative isohydric plant, whose exploit middle and deep soil water sources may render it more vulnerable under future drought intensification and soil salinization aggrandizement. This coordination between water-use pattern and physiological traits provides a valuable framework for understanding species-specific drought resilience in water-limited ecosystems.

explain Tamarix chinensis and Ulmus pumila divergent water use strategies.

4.4 Implication for forest management in saline-alkaline ecosystem

The Yellow River Delta is a unique coastal ecosystem where vegetation growth is constrained by shallow groundwater tables, high soil salinity, and strong seasonal variability in precipitation (Liu et al., 2018; Xia et al., 2019; Zhang et al., 2022). Prolonged droughts exacerbate salt accumulation in the upper soil layers through enhanced evaporation, while freshwater scarcity limits leaching, creating a dual stress of salinity and water deficit for plant survival (Hassani et al., 2021; Chen et al., 2022). In this context, understanding the contrasting water-use strategies of *T. chinensis* and *U. pumila* offers valuable guidance for afforestation and restoration planning in saline-alkaline environments.

Our study shows that *U. pumila* adopts an isohydric strategy, maintaining stable leaf water potentials through tight stomatal control and a consistent dependence on intermediate and deep soil water. This conservative water use strategy reduces hydraulic risk but tends to be more vulnerable to water stress especially in the highly seasonal precipitation regimes of the Yellow River Delta. First, the isohydric behavior of *U. pumila* indicates reliance on carbohydrate reserves to satisfy carbon requirements for respiration and osmoregulation. Continuous metabolic demand may progressively deplete these reserves, ultimately resulting in carbon starvation (McDowell et al., 2008; Skelton et al., 2015; Kono et al., 2019). Such depletion progressively undermines drought resilience, reducing stand productivity and ecosystem health (Adams et al., 2017; Hartmann et al., 2018). Besides, overreliance on a single water source can intensify hydrological trade-offs, amplifying water acquisition challenges when that source is depleted (Yin et al., 2024). Consequently, Although *U. pumila*'s isohydric behavior may provide an adaptive strategy to survive in water-limited environment, the long-term viability of this strategy is questionable. Balancing ecological benefits with hydrological sustainability requires optimizing planting densities and implementing rigorous monitoring of deep soil water reserves.

T. chinensis demonstrates high ecological plasticity through its anisohydric behavior and flexible shifts in water uptake between shallow, deep, and groundwater in response to water variability. This adaptability sustains higher gas exchange during drought and

allows exploitation of deep soil water reserves when surface soils desiccate or salinity rises. These traits that position *T. chinensis* as a key species for revegetating degraded saline-alkaline zones, particularly in drought-prone regions. Notably, *T. chinensis* outcompetes *U. pumila* in such environments by flexible shifting in water uptake, supporting superior productivity during seasonal water fluctuations. Although anisohydric plants may face a higher risk of hydraulic failure, their flexibility in water sourcing enables them to sustain relatively greater water acquisition (Martínez-Vilalta and Garcia-Forner, 2017; Walthert et al., 2024). This adaptable water-use strategy is likely to confer greater advantages under the anticipated increase in drought frequency and will promote tree's survival probability (Muñoz-Gálvez et al., 2024).

Our study reveals a tight coordination between dynamic water source partitioning and distinct iso-/anisohydric behaviors in two dominant tree species under saline-alkaline stress. This integrated approach addresses a critical gap by uncovering the mechanistic link between root water uptake and stomatal regulation in salinealkaline soils, thereby providing a more holistic understanding of their drought adaptation strategies. Our results suggest that afforestation and restoration in the Yellow River Delta should account for the interaction between species-specific water-use strategies, soil salinity dynamics, and water availability. T. chinensis appears better suited than U. pumila for initiating revegetation in the Yellow River Delta. T. chinensis, with its anisohydric behavior and flexible water uptake strategy, should be prioritized for afforestation in areas with high seasonal variability in precipitation and soil salinity. Its ability to utilize deeper, more saline water sources confers greater resilience to drought. U. pumila may be better suited for planting in areas with more reliable freshwater availability or in mixed-species plantations. Its isohydric conservatism could be complemented by the plasticity of species like T. chinensis, potentially enhancing overall ecosystem stability and resource partitioning. Nevertheless, determining an optimal planting density may be necessary to avoid excessive depletion of deep soil water resources. Aligning forest management with species-specific water-use strategies, such as the anisohydric plasticity of T. chinensis versus the isohydric conservatism of U. pumila, is crucial for enhancing drought resilience in seasonally arid forests.

5 Conclusion

Differences in water uptake patterns and physiological responses were observed between *T. chinensis* and. *U. pumila*. *T. chinensis* employs a plastic water uptake strategy, dynamically shifting soil water acquisition depths in response to seasonal aridity, whereas *U. pumila* maintains a conservative water-use strategy characterized by stable dependence on predictable moisture reservoirs throughout the growing season. *T. chinensis* is an anisohydric species, as characterized by a greater diurnal water

potential range and a lack of significant correlation between gs and water potential (p>0.05). In contrast, the isohydric *U. pumila* had a more conservative strategy, tightly regulating transpiration by closing stomata in response to declining leaf water potential (p<0.05). The water uptake patterns of T. chinensis and U. pumila are tightly coordinated with their respective iso-/anisohydric behaviors and associated physiological traits. T. chinensis facilitates access to more stable, deeper water reserves to sustain stomatal opening and declined water potential. The physiological characteristics of *U. pumila*, in conjunction with isohydric regulation, maintain leaf water potential under drought conditions by restricting water uptake exclusively to the relatively stable and low-salinity middle and deep soil layers. Our findings demonstrate that, for saline-alkali soils, T. chinensis's water-use strategy conveys stronger adaptive advantages under shifting precipitation regimes. Aligning forest management with speciesspecific water-use strategies, such as the anisohydric plasticity of *T*. chinensis versus the isohydric conservatism of U. pumila, is crucial for enhancing drought resilience in seasonally arid forests.

Data availability statement

The raw data supporting the conclusions of this article will be made available by the authors, without undue reservation.

Author contributions

TW: Software, Writing – original draft, Data curation, Methodology. CD: Writing – review & editing, Investigation, Software. HW: Investigation, Writing – review & editing. RZ: Writing – review & editing. Investigation. RR: Software, Writing – review & editing. SY: Writing – review & editing. XX: Formal analysis, Writing – review & editing, Supervision, Conceptualization.

Funding

The author(s) declare financial support was received for the research and/or publication of this article. This work was financially supported by the National Natural Science Foundation of China (32301574), Shandong Provincial Natural Science Foundation (ZR2023QC134) and the Open Project of Liaocheng University Landscape Architecture Discipline (319462212).

Acknowledgments

We also thank the Comprehensive Experimental Center in Yellow River Delta of Chinese Academy of Forestry for their support in our field work.

Conflict of interest

The authors declare that the research was conducted in the absence of any commercial or financial relationships that could be construed as a potential conflict of interest.

Generative AI statement

The author(s) declare that no Generative AI was used in the creation of this manuscript.

Any alternative text (alt text) provided alongside figures in this article has been generated by Frontiers with the support of artificial

intelligence and reasonable efforts have been made to ensure accuracy, including review by the authors wherever possible. If you identify any issues, please contact us.

Publisher's note

All claims expressed in this article are solely those of the authors and do not necessarily represent those of their affiliated organizations, or those of the publisher, the editors and the reviewers. Any product that may be evaluated in this article, or claim that may be made by its manufacturer, is not guaranteed or endorsed by the publisher.

References

Adams, H. D., Zeppel, M. J. B., Anderegg, W. R. L., Hartmann, H., Landhäusser, S. M., Tissue, D. T., et al. (2017). A multi-species synthesis of physiological mechanisms in drought-induced tree mortality. *Nat. Ecol. Evol.* 1, 1285–1291. doi: 10.1038/s41559-017-0248-x

Bachofen, C., Tumber-Dávila, S. J., Mackay, D. S., McDowell, N. G., Carminati, A., Klein, T., et al. (2024). Tree water uptake patterns across the globe. *New Phytol.* 242, 1891–1910. doi: 10.1111/nph.19762

Barbeta, A., Jones, S. P., Clavé, L., Wingate, L., Gimeno, T. E., Fréjaville, B., et al. (2019). Unexplained hydrogen isotope offsets complicate the identification and quantification of tree water sources in a riparian forest. *Hydrol Earth Syst. Sci.* 23, 2129–2146. doi: 10.5194/hess-23-2129-2019

Barbeta, A., Mejía-Chang, M., Ogaya, R., Voltas, J., Dawson, T. E., and Peñuelas, J. (2015). The combined effects of a long-term experimental drought and an extreme drought on the use of plant-water sources in a Mediterranean forest. *Glob. Change Biol.* 21, 1213–1225. doi: 10.1111/gcb.12785

Chen, P., Xia, J., Ma, H., Gao, F., Dong, M., Xing, X., et al. (2022). Analysis of spatial distribution pattern and its influencing factors of the Tamarix chinensis population on the beach of the muddy coastal zone of Bohai Bay. *Ecol. Indic.* 140, 109016. doi: 10.1016/j.ecolind.2022.109016

Dawson, T. E., and Ehleringer, J. R. (1991). Streamside trees that do not use stream water. $Nature\ 350,\ 335-337.\ doi:\ 10.1038/350335a0$

Dawson, T. E., and Pate, J. S. (1996). Seasonal water uptake and movement in root systems of Australian phraeatophytic plants of dimorphic root morphology: a stable isotope investigation. *Oecologia* 107, 13–20. doi: 10.1007/BF00582230

Ding, Y., Nie, Y., Chen, H., Wang, K., and Querejeta, J. I. (2021). Water uptake depth is coordinated with leaf water potential, water-use efficiency and drought vulnerability in karst vegetation. *New Phytol.* 229, 1339–1353. doi: 10.1111/nph.16971

Ehleringer, J. R., and Dawson, T. E. (1992). Water uptake by plants: perspectives from stable isotope composition. *Plant Cell Environ.* 15, 1073–1082. doi: 10.1111/j.1365-3040.1992.tb01657.x

Ewe, S. M. L., Sternberg, L., da, S. L., and Childers, D. L. (2007). Seasonal plant water uptake patterns in the saline southeast Everglades ecotone. *Oecologia* 152, 607–616. doi: 10.1007/s00442-007-0699-x

Franks, P. J., Drake, P. L., and Froend, R. H. (2007). Anisohydric but isohydrodynamic: seasonally constant plant water potential gradient explained by a stomatal control mechanism incorporating variable plant hydraulic conductance. *Plant Cell Environ.* 30, 19–30. doi: 10.1111/j.1365-3040.2006.01600.x

Gessler, A., Bächli, L., Rouholahnejad Freund, E., Treydte, K., Schaub, M., Haeni, M., et al. (2022). Drought reduces water uptake in beech from the drying topsoil, but no compensatory uptake occurs from deeper soil layers. *New Phytol.* 233, 194–206. doi: 10.1111/nph.17767

Grossiord, C., Sevanto, S., Dawson, T. E., Adams, H. D., Collins, A. D., Dickman, L. T., et al. (2017). Warming combined with more extreme precipitation regimes modifies the water sources used by trees. *New Phytol.* 213, 584–596. doi: 10.1111/nph.14192

Hartmann, H., Moura, C. F., Anderegg, W. R. L., Ruehr, N. K., Salmon, Y., Allen, C. D., et al. (2018). Research frontiers for improving our understanding of drought-induced tree and forest mortality. *New Phytol.* 218, 15–28. doi: 10.1111/nph.15048

Hassani, A., Azapagic, A., and Shokri, N. (2021). Global predictions of primary soil salinization under changing climate in the 21st century. *Nat. Commun.* 12, 6663. doi: 10.1038/s41467-021-26907-3

He, X., Hui, D., Liu, H., Wang, F., Yao, K., Lu, H., et al. (2024). Responses of plant water uptake sources to altered precipitation patterns in a tropical secondary forest. *Agric. For. Meteorol.* 355, 110138. doi: 10.1016/j.agrformet.2024.110138

Hochberg, U., Rockwell, F. E., Holbrook, N. M., and Cochard, H. (2018). Iso/ anisohydry: A plant–environment interaction rather than a simple hydraulic trait. *Trends Plant Sci.* 23, 112–120. doi: 10.1016/j.tplants.2017.11.002

Imada, S., Matsuo, N., Acharya, K., and Yamanaka, N. (2015). Effects of salinity on fine root distribution and whole plant biomass of Tamarix ramosissima cuttings. *J. Arid Environ.* 114, 84–90. doi: 10.1016/j.jaridenv.2014.11.011

Jiang, P., Wang, H., Meinzer, F. C., Kou, L., Dai, X., and Fu, X. (2020). Linking reliance on deep soil water to resource economy strategies and abundance among coexisting understorey shrub species in subtropical pine plantations. *New Phytol.* 225, 222–233. doi: 10.1111/nph.16027

Kannenberg, S. A., Novick, K. A., and Phillips, R. P. (2019). Anisohydric behavior linked to persistent hydraulic damage and delayed drought recovery across seven North American tree species. *New Phytol.* 222, 1862–1872. doi: 10.1111/nph.15699

Kono, Y., Ishida, A., Saiki, S.-T., Yoshimura, K., Dannoura, M., Yazaki, K., et al. (2019). Initial hydraulic failure followed by late-stage carbon starvation leads to drought-induced death in the tree Trema orientalis. *Commun. Biol.* 2, 8. doi: 10.1038/s42003-018-0256-7

Landwehr, J. M., and Coplen, T. B. (2006). Line-conditioned excess: a new method for characterizing stable hydrogen and oxygen isotope ratios in hydrologic systems, in *Isotopes in Environmental Studies*, (Vienna: International Atomic Energy Agency), 132–135.

Lei, S., Jia, X., Zhao, C., and Shao, M. (2025). A review of saline-alkali soil improvements in China: Efforts and their impacts on soil properties. *Agric. Water Manage.* 317, 109617. doi: 10.1016/j.agwat.2025.109617

Li, W., Migliavacca, M., Forkel, M., Denissen, J. M. C., Reichstein, M., Yang, H., et al. (2022). Widespread increasing vegetation sensitivity to soil moisture. *Nat. Commun.* 13, 3959. doi: 10.1038/s41467-022-31667-9

Li, Y., Ma, Y., Song, X., Wang, L., and Han, D. (2021). A δ2H offset correction method for quantifying root water uptake of riparian trees. *J. Hydrol.* 593, 125811. doi: 10.1016/j.jhydrol.2020.125811

Lin, G., and Sternberg, da S.L.L. (1993). "31 - hydrogen isotopic fractionation by plant roots during water uptake in coastal wetland plants," in *Stable Isotopes and Plant Carbon-water Relations*. Eds. J. R. Ehleringer, A. E. Hall and G. D. Farquhar (Academic Press, San Diego), 497–510. doi: 10.1016/B978-0-08-091801-3.50041-6

Liu, S., Hou, X., Yang, M., Cheng, F., Coxixo, A., Wu, X., et al. (2018). Factors driving the relationships between vegetation and soil properties in the Yellow River Delta, China. *Catena* 165, 279–285. doi: 10.1016/j.catena.2018.02.004

Liu, Z., Yu, X., and Jia, G. (2019). Water uptake by coniferous and broad-leaved forest in a rocky mountainous area of northern China. *Agric. For. Meteorol.* 265, 381–389. doi: 10.1016/j.agrformet.2018.11.036

Martínez-Vilalta, J., and Garcia-Forner, N. (2017). Water potential regulation, stomatal behavior and hydraulic transport under drought: deconstructing the iso/anisohydric concept. *Plant Cell Environ.* 40, 962–976. doi: 10.1111/pce.12846

Martín-Gómez, P., Aguilera, M., Pemán, J., Gil-Pelegrín, E., and Ferrio, J. P. (2017). Contrasting ecophysiological strategies related to drought: the case of a mixed stand of Scots pine (Pinus sylvestris) and a submediterranean oak (Quercus subpyrenaica). *Tree Physiol.* 37, 1478–1492. doi: 10.1093/treephys/tpx101

McDowell, N., Pockman, W. T., Allen, C. D., Breshears, D. D., Cobb, N., Kolb, T., et al. (2008). Mechanisms of plant survival and mortality during drought: why do some plants survive while others succumb to drought? *New Phytol.* 178, 719–739. doi: 10.1111/j.1469-8137.2008.02436.x

Meinzer, F. C., Woodruff, D. R., Marias, D. E., Smith, D. D., McCulloh, K. A., Howard, A. R., et al. (2016). Mapping 'hydroscapes' along the iso- to anisohydric continuum of stomatal regulation of plant water status. *Ecol. Lett.* 19, 1343–1352. doi: 10.1111/ele.12670

Miguez-Macho, G., and Fan, Y. (2021). Spatiotemporal origin of soil water taken up by vegetation. *Nature* 598, 624–628. doi: 10.1038/s41586-021-03958-6

Min, X.-J., Zang, Y.-X., Sun, W., and Ma, J.-Y. (2019). Contrasting water sources and water-use efficiency in coexisting desert plants in two saline-sodic soils in northwest China. *Plant Biol.* 21, 1150–1158. doi: 10.1111/plb.13028

Morgan, B. E., Araki, R., Trugman, A. T., and Caylor, K. K. (2025). Ecological and hydroclimatic determinants of vegetation water-use strategies. *Nat. Ecol. Evol.* 9, 1791–1799. doi: 10.1038/s41559-025-02810-8

Muñoz-Gálvez, F. J., Querejeta, J. I., Moreno-Gutiérrez, C., Ren, W., Riva, E. G. D. L., and Prieto, I. (2024). Trait coordination and trade-offs constrain the diversity of water use strategies in Mediterranean woody plants. 16, 4103. doi: 10.21203/rs.3.rs-4780630/v1

Skelton, R. P., West, A. G., and Dawson, T. E. (2015). Predicting plant vulnerability to drought in biodiverse regions using functional traits. *Proc. Natl. Acad. Sci.* 112, 5744–5749. doi: 10.1073/pnas.1503376112

Stock, B. C., and Semmens, B. X. (2013). MixSIAR GUI User Manual, Version 3.1. Available online at: http://conserver.iugocafe.org/user/brice.semmens/MixSIAR (Accessed October 3, 2024).

Sun, J., Xia, J., Shao, P., Ma, J., Gao, F., Lang, Y., et al. (2022). Response of the fine root morphological and chemical traits of Tamarix chinensis to water and salt changes in coastal wetlands of the Yellow River Delta. *Front. Plant Sci.* 13. doi: 10.3389/fpls.2022.952830

Sun, J., Xia, J., Zhao, X., Gao, F., Zhao, W., Xing, X., et al. (2023). Enrichment of soil nutrients and salt ions with different salinities under Tamarix chinensis shrubs in the Yellow River Delta. *Catena* 232, 107433. doi: 10.1016/j.catena.2023.107433

Walthert, L., Etzold, S., Carminati, A., Saurer, M., Köchli, R., and Zweifel, R. (2024). Coordination between degree of isohydricity and depth of root water uptake in temperate tree species. *Sci. Total Environ.* 946, 174346. doi: 10.1016/j.scitotenv.2024.174346

Wang, J., Fu, B., Lu, N., and Zhang, L. (2017). Seasonal variation in water uptake patterns of three plant species based on stable isotopes in the semi-arid Loess Plateau. *Sci. Total Environ.* 609, 27–37. doi: 10.1016/j.scitotenv.2017.07.133

Wang, T., Xu, Q., Zhang, B., Gao, D., Zhang, Y., Jiang, J., et al. (2024). Effects of thinning and understory removal on water use efficiency of Pinus massoniana: evidence from photosynthetic capacity and stable carbon isotope analyses. *J. For. Res.* 35, 41. doi: 10.1007/s11676-023-01666-7

Wang, T., Xu, Q., Zhang, B., Gao, D., Zhang, Y., Ren, R., et al. (2022). Effects of understory removal and thinning on water uptake patterns in Pinus massoniana Lamb. plantations: Evidence from stable isotope analysis. *For. Ecol. Manage.* 503, 119755. doi: 10.1016/j.foreco.2021.119755

Xia, J., Ren, J., Zhang, S., Wang, Y., and Fang, Y. (2019). Forest and grass composite patterns improve the soil quality in the coastal saline-alkali land of the Yellow River Delta, China. *Geoderma* 349, 25–35. doi: 10.1016/j.geoderma.2019.04.032

Xue, J., Huete, A., Liu, Z., Wang, Y., and Lu, X. (2024). Estimation of global ecosystem isohydricity from solar-induced chlorophyll fluorescence and meteorological datasets. *Remote Sens. Environ.* 307, 114168. doi: 10.1016/irse.2024.114168

Yang, B., Wen, X., and Sun, X. (2015). Seasonal variations in depth of water uptake for a subtropical coniferous plantation subjected to drought in an East Asian monsoon region. *Agric. For. Meteorol.* 201, 218–228. doi: 10.1016/j.agrformet.2014.11.020

Yin, D., Gou, X., Liu, J., Zhang, D., Wang, K., and Yang, H. (2024). Increasing deep soil water uptake during drought does not indicate higher drought resistance. *J. Hydrol.* 630, 130694. doi: 10.1016/j.jhydrol.2024.130694

Zhang, L., Lan, S., Zhao, L., Yi, H., and Han, G. (2022). Temporal variation of wateruse efficiency and water sources of Phragmites australis in the coastal wetland: Based on stable isotopic composition (δ 13C and δ 18O). *Ecol. Indic.* 139, 108957. doi: 10.1016/j.ecolind.2022.108957

Zhang, B., Xu, Q., Liu, S., Gu, B., Gao, D., Wang, T., et al. (2024). Unraveling the effects of plant and soil properties on tree water absorption in pure and mixed forests across subtropical China. *Agric. For. Meteorol.* 353, 110078. doi: 10.1016/j.agrformet.2024.110078

Zhao, Y., Wang, Y., He, M., Tong, Y., Zhou, J., Guo, X., et al. (2020). Transference of Robinia pseudoacacia water-use patterns from deep to shallow soil layers during the transition period between the dry and rainy seasons in a water-limited region. For. Ecol. Manage. 457, 117727. doi: 10.1016/j.foreco.2019.117727

Zhao, Y., Wang, L., Knighton, J., Evaristo, J., and Wassen, M. (2021). Contrasting adaptive strategies by Caragana korshinskii and Salix psammophila in a semiarid revegetated ecosystem. *Agric. For. Meteorol.* 300, 108323. doi: 10.1016/j.agrformet.2021.108323

Zhu, J., Liu, J., Li, J., Zhao, C., and Sun, J. (2022). Water uptake tradeoffs of dominant shrub species in the coastal wetlands of the yellow river delta, China. *Front. Plant Sci.* 13. doi: 10.3389/fpls.2022.935025